AD-A208 078

REPORT DOCUMENTATION PAGE

1a. REPORT SECURITY CLASSIFICATION: UNCLASSIFIED	1b. RESTRICTIVE MARKINGS
2a. SECURITY CLASSIFICATION AUTHORITY	3. DISTRIBUTION/AVAILABILITY OF REPORT: Approved for public release; distribution is unlimited.
2b. DECLASSIFICATION/DOWNGRADING SCHEDULE	
4. PERFORMING ORGANIZATION REPORT NUMBER(S)	5. MONITORING ORGANIZATION REPORT NUMBER(S)
6a. NAME OF PERFORMING ORGANIZATION: Naval Ocean Systems Center; 6b. OFFICE SYMBOL (If applicable): NOSC	7a. NAME OF MONITORING ORGANIZATION
6c. ADDRESS (City, State and ZIP Code): San Diego, CA 92152-5000	7b. ADDRESS (City, State and ZIP Code)
8a. NAME OF FUNDING/SPONSORING ORGANIZATION: Director of Naval Laboratories; 8b. OFFICE SYMBOL (If applicable): DNL	9. PROCUREMENT INSTRUMENT IDENTIFICATION NUMBER
8c. ADDRESS (City, State and ZIP Code): Space and Naval Warfare Systems Command, Washington, DC 20360	10. SOURCE OF FUNDING NUMBERS: PROGRAM ELEMENT NO. 0601152N; PROJECT NO. ZT86; TASK NO. RR00N00; AGENCY ACCESSION NO. DN308 045

11. TITLE (Include Security Classification)

VALENCE, CHARGE TRANSFER AND CARRIER TYPE FOR $Bi_2Sr_2Ca_{n-1}Cu_nO_{2n+4+\delta}$ AND RELATED HIGH TEMPERATURE CERAMIC SUPERCONDUCTORS

12. PERSONAL AUTHOR(S)

T. E. Jones, W. C. McGinnis, R. D. Boss, E. W. Jacobs, J. W. Schindler, C. D. Rees

13a. TYPE OF REPORT	13b. TIME COVERED	14. DATE OF REPORT (Year, Month, Day)	15. PAGE COUNT
Professional paper	FROM Sep 1988 TO Sep 1988	March 1989	

16. SUPPLEMENTARY NOTATION

17. COSATI CODES			18. SUBJECT TERMS (Continue on reverse if necessary and identify by block number)
FIELD	GROUP	SUB-GROUP	thin films, superconductivity, ceramic, copper oxides, Bismuth compounds, Calcium/Strontium compounds, reprints

19. ABSTRACT (Continue on reverse if necessary and identify by block number)

Samples of the bismuth-based high temperature superconducting family $Bi_2Sr_2Ca_{n-1}Cu_nO_{2n+4+\delta}$ have been prepared and characterized by x-ray diffraction, and temperature-dependent resistivity and thermoelectric power measurements. Both of the high temperature superconducting phases reported in the literature, with transition temperatures near 80K and 110K, have been observed. Evidence from thermoelectric power measurements is presented which shows that this family of ceramic superconductors has contributions to the electrical transport that is both electron-like and hole-like. However, all of the superconducting transitions observed involve hole-like states.

89 5 24 063

Presented at the American Chemical Society, 25 - 30 Sep 1988, Los Angeles, CA. Published 1988 American Chemical Society.

20. DISTRIBUTION/AVAILABILITY OF ABSTRACT	21. ABSTRACT SECURITY CLASSIFICATION	
[X] UNCLASSIFIED/UNLIMITED [ ] SAME AS RPT [ ] DTIC USERS	UNCLASSIFIED	
22a. NAME OF RESPONSIBLE PERSON: T. E. Jones	22b. TELEPHONE (Include Area Code): (619) 553-1594	22c. OFFICE SYMBOL: Code 633

DD FORM 1473, 84 JAN

83 APR EDITION MAY BE USED UNTIL EXHAUSTED
ALL OTHER EDITIONS ARE OBSOLETE

UNCLASSIFIED
SECURITY CLASSIFICATION OF THIS PAGE

Chapter 13

Valence, Charge Transfer, and Carrier Type for $Bi_2Sr_2Ca_{n-1}Cu_nO_{2n+4+\delta}$ and Related High-Temperature Ceramic Superconductors

T. E. Jones, W. C. McGinnis, R. D. Boss, E. W. Jacobs, J. W. Schindler, and C. D. Rees

Naval Ocean Systems Center, Code 633, San Diego, CA 92152–5000

Samples of the bismuth-based high temperature superconducting family $Bi_2Sr_2Ca_{n-1}Cu_nO_{2n+4+\delta}$ have been prepared and characterized by x-ray diffraction, and temperature-dependent resistivity and thermoelectric power measurements. Both of the high temperature superconducting phases reported in the literature, with transition temperatures near 80K and 110K, have been observed. Evidence from thermoelectric power measurements is presented which shows that this family of ceramic superconductors has contributions to the electrical transport that is both electron-like and hole-like. However, all of the superconducting transitions observed involve hole-like states.

With the recent discovery of the new high temperature ceramic superconductors based on both bismuth (1,2) and thallium (3,4), there is renewed interest in the electronic states of these materials and, in particular, the charge transfer to and from the Cu-O planes vis-a-vis the $YBa_2Cu_3O_7$ family. With no Cu-O chains in the bismuth (5) and thallium (4) materials, the role of the Bi-O and Tl-O planes is being investigated via thermoelectric measurements. The absolute thermoelectric power (thermopower) of a material generally yields the sign of the dominant charge carrier and, as in Hall effect measurements, distinguishes between electron-like (n-type carriers) and hole-like (p-type carriers) conduction. In the previous high temperature superconductors, $(La,Sr)_2CuO_4$ and $YBa_2Cu_3O_7$, both the normal state conductivity and the superconductivity have been shown to be due to hole-like states (6,7). In the lanthanum material, doping with a divalent element, barium or strontium, in place of the trivalent lanthanum, effectively removes electrons from the Cu-O planes leaving conducting hole-like states. Also, x-ray photoemission

spectroscopy (8,9) shows that doping creates holes in the Cu-O planes. However, in the heavily doped lanthanum material (25% strontium replacement), evidence from thermoelectric power measurements extended above room temperature have been reported which suggest that there is also a contribution to the normal conductivity from electrons (6). In the yttrium material, empirical atom-atom potential calculations (10,11), extended Hückel molecular orbital calculations (12) and bond-valence calculations (13) imply electron transfer from the Cu-O planes to the Cu-O chains. In addition, the results of substitutional studies with zinc and gallium by Xiau et al. (14), show that it is the Cu-O planes which are important for superconductivity, rather than the Cu-O chains, in $YBa_2Cu_3O_7$.

In the bismuth family of materials, one could argue that electrons may be transferred from the Bi-O planes to the Cu-O planes. Because bismuth presumably goes into the material in the valence +3 state, partial conversion to bismuth +5 would require hole states on the bismuth planes and electron states on the Cu-O planes. If such electron transfer occurs and the charge carriers in these materials reside on the Cu-O planes (as in the other copper oxide superconductors), then conduction would be due to n-type electronic states. This would be quite different than in the other copper oxide high temperature superconducting ceramics, where the superconductivity comes from paired hole states. On the other hand, band structure calculations of Hybertsen and Mattheiss indicate that the Bi-O planes in effect dope the Cu-O planes with additional holes, that is, that electrons are transferred from the Cu-O planes to the Bi-O planes (15). Assuming these calculations are correct, there may be an n-type contribution to the conductivity from the Bi-O planes, but the superconductivity would be very similar to that observed in all other copper oxide superconducting ceramics to date, that is, due to pairing of holes in the Cu-O planes.

These considerations have provided the motivation for the experiments described in this paper. Specifically, we would like to answer two questions: Is the conduction in the bismuth family of superconductors due to electrons or holes, and which carriers condense into the superconducting state at each of the observed superconducting transitions in the bismuth family?

Sample Preparation and Characterization

Samples were prepared from Y_2O_3 (Aesar, 99.99%), $BaCO_3$ (Aesar, 99.997%), CuO (Aesar, 99.999%), Bi_2O_3 (Aesar, 99.9998%), $SrCO_3$ (Aesar, 99.999%), and $CaCO_3$ (Aesar, 99.9995%), all of which were used as received. The $YBa_2Cu_3O_7$, sample 1, was prepared from the constituent oxides and $BaCO_3$. The powders were mixed and calcined at 950°C for 16 hours in air, ball-milled to a fine powder, pressed into pellets and sintered at approximately 955°C for 12

hours in oxygen. It was then cooled at 2°C/min. to approximately 550°C in oxygen, annealed at 550°C for 6 hours in oxygen, cooled to 350°C at 2°C/min. in oxygen, and furnace cooled to 200°C in oxygen.

Samples 2-5 were prepared with nominal compositions of Bi:Sr:Ca:Cu in the molar ratios of 2:2:1:2, 2:2:2:3, 4:3:3:6, and 4:3:3:6, respectively. Samples 2 and 3 were calcined in porcelain crucibles for 5 hours at 860°C, then ground and pressed into pellets which were then baked on alumina disks at 860°C for 86 hours. Sample 3 was then baked for an additional 72 hrs at 875°C.

Samples 4 and 5 were calcined for 12 hours at 860°C, ground, then recalcined at 860°C for 12 more hours. After regrinding and pressing into pellets, the pellets were baked on an alumina disk at 865°C for 65 hours in air, concluding with a slow cool in oxygen. This material was then baked further in air for 41 hours at 880°C. During this 880°C bake the sample material reacted to produce a bronze colored coating on the exposed surfaces and reacted with the alumina substrate to produce a green colored material. This green material formed small stalagmites which lifted the pellets about 1 mm above the alumina disk. The crystalline-appearing pellet material supported by the stalagmites constitutes sample 4, with properties reported in this paper. The green stalagmite material is being chemically analyzed. Sample 5 was processed as number 4, but with 70 hours of additional furnace time at 880°C. This sample resembled sample 4 but it also had a glossy black crystalline appearing surface.

All samples were characterized by powder x-ray diffraction, using Cu K-α radiation on material taken from each pellet after all processing. The diffraction pattern for sample 1 agrees with literature data for the yttrium 1:2:3 layered perovskite structure. The diffraction patterns for samples 2-4 are shown in Figure 1. The pattern for sample 3 is in excellent agreement with those of Tarascon *et al.* (5) and Takayama-Muromachi *et al.* (2). Therefore, we believe sample 3 is mostly $Bi_2Sr_2Ca_{n-1}Cu_nO_{2n+4+\delta}$ with n=2. While all three patterns are similar there are some differences, which may be reflective of the basic differences in the electrical properties of the samples. It should also be noted that a diffraction pattern from sample 4 taken prior to the final 880°C bake was essentially equivalent to that of sample 3, with the exception of a large peak at an angle 2θ=32°.

An examination of sample 2 with an optical microscope shows no apparent crystallinity on that scale. Similarly, sample 3 shows little bulk crystallinity on an optical scale, but several small domains of microcrystallinity were dispersed throughout the material. The appearance of both samples 2 and 3 were independent of whether or not the surface had been in contact with the alumina substrate. Conversely, samples 4 and 5 had different appearances for the surface in contact with the alumina and the other surfaces. The surface which was in contact with the alumina was black but essentially microcrystalline everywhere. Microscopy of the other surfaces revealed small golden colored bars, with the remaining area being black in coloration. It is also of note that the surface in contact with the alumina had, prior to

the final 880°C bake, grown flat plate-like whiskers which were not present after the 880°C bake. The stalagmite-like formations were not very crystalline visually, and contained regions of various colors.

Electronic Properties

Each of the five samples described above were shaped with hand tools into rectangular bars approximately 2 mm x 2 mm x 4 mm. They were mounted in a closed-cycle He-4 refrigerator in such a way that the thermopower and four-probe resistance of all samples could be measured during a single cooling/warming cycle. This arrangement is shown schematically in Figure 2.

The thermopower data was obtained using a slow a.c. differential technique (16) in which a small, slowly oscillating thermal gradient is produced across the sample, and the resultant thermoelectric voltage measured at the sample ends. The temperature gradient was produced by alternately heating two parallel quartz blocks (each wrapped with Manganin wire heaters) which were bridged by the samples. The blocks were bonded (using G.E. 7031 varnish) to a brass sheet, which was in turn attached (with a thin layer of Apiezon N grease) to the copper stage on the cold-head of the refrigerator. The temperature T_{stage} of the refrigerator stage was monitored with a calibrated silicon diode. The samples were soldered, along with the thermoelectric voltage leads (#34 copper; Belden 8057), to the edges of the quartz blocks with indium. The temperature difference ΔT between the two quartz blocks (that is, the temperature drop across the sample) was measured using a copper/constantan/copper differential thermocouple whose junctions were indium soldered to the quartz. The time-averaged temperature difference δT between one of the quartz blocks and the refrigerator stage was also monitored with this type of thermocouple. The average sample temperature T is then given by $T_{stage} + \delta T$.

At a given temperture, the thermopower of each sample was measured as follows. The voltage of the block-to-block thermocouple was plotted on an X-Y recorder versus the thermoelectric voltage measured across the sample, ΔV, as the blocks were alternately heated at a frequency which varied with temperature, but which was in the range of 0.02-0.05 Hz. The thermocouple voltages were converted to a temperature difference using tabulated values (17) of $dV/dT = S_{constantan} - S_{Cu}$. The resultant trace, apart from transient behavior as the heater current was switched from one quartz block to the other, was a straight line whose temperature-converted slope, $\Delta V/\Delta T$, equals the sample thermopower minus the thermopower of the copper voltage leads. After the heating current is switched to the other block, the trace is completed to form a closed loop. The block-to-block temperature difference, ΔT, was usually less than 1K.

Normally, the thermopower measurements would be performed at a constant T_{stage}. It was more convenient, however, to take mea-

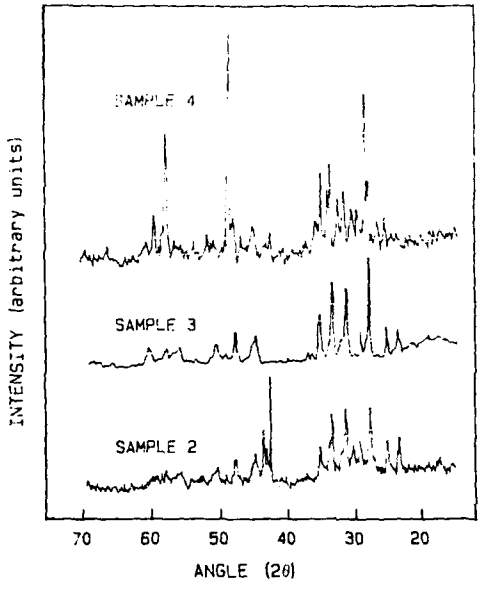

Figure 1. X-ray scans for samples 2-4.

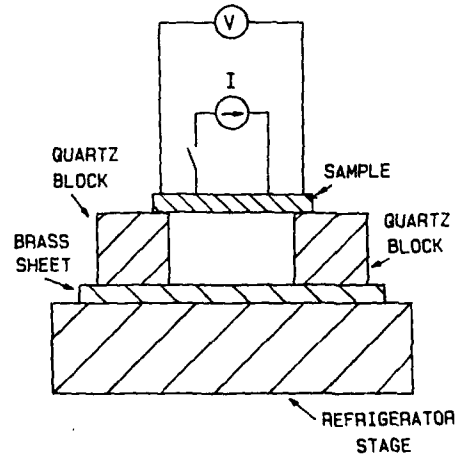

Figure 2. The apparatus for measuring the thermopower.

surements while the refrigerator, which was continually pumped by a liquid nitrogen trapped diffusion pump, very slowly warmed at a rate of about 0.5 K/min. As a typical trace required about 30 seconds to complete, this mode of operation introduced very little error and greatly sped data acquisition. Before each set of thermopower traces at a given temperature, readings of the four-probe resistance were taken by closing the current source switch shown in Figure 2. For convenience, the current was sent through the center connections on the samples (using the same type of wire as the voltage leads) and the voltage measured at the end connections. Reversing the current and voltage leads gave the same resistance values. Within experimental accuracy, the thermopower values measured with and without the current wires attached to the samples were the same.

The temperature dependent thermopower of the copper voltage leads is required in order to obtain the samples' absolute thermopower. For temperatures below 91K, sample 1 is superconducting and therefore has zero thermopower, which allowed a direct determination of the absolute thermopower of the copper voltage leads. The copper thermopower values from this self-calibration agree with the results of Crisp et al. (18), as corrected by the new thermopower scale of Roberts (19), throughout this temperature range. The values of S_{Cu} used to analyze the thermopower data of the samples were a composite of a fit to the voltage lead data taken on sample 1, for $T < 91K$, and the high temperature data of Crisp et al., for $T > 91K$.

Errors in thermopower measurements can arise from several sources. The main source of error in this experimental configuration was an approximately 10% uncertainty in the temperature difference ΔT across the samples due to uneven heating of the quartz blocks. For temperatures above 91K, values of the samples' absolute thermopower may be off by as much as 0.25 $\mu V/K$, depending on the values of S_{Cu} used. The error in the sample temperature T was relatively small, approximately $\pm 0.3K$. The resistivity data contain a fixed error of about 10% due to uncertainty in the measured sample dimensions.

Results of the thermopower and resistance measurements for samples 1-4 are displayed in Figures 3-6, respectively. In Figure 3, the $YBa_2Cu_3O_7$ resistivity data show the usual superconducting transition at 94K. The thermopower for this sample is positive above this temperature, indicating hole-like carriers, and drops to zero at the transition. The data are very similar to that obtained by Uher et al. (7) As shown in Figure 4, the thermopower and resistivity of sample 2 both vanish at approximately 80K. The thermopower reaches its maximum positive value just above the superconducting transition, and decreases from there with rising temperature. The thermopower changes sign from positive to negative at about 200K, indicating that electrons become the dominant carriers above this temperature. Figure 5 shows that the thermopower and resistivity of sample 3 both go to zero at about 90K. In contrast to sample 2, holes appear to be the dominant carrier throughout the temperature range investigated.

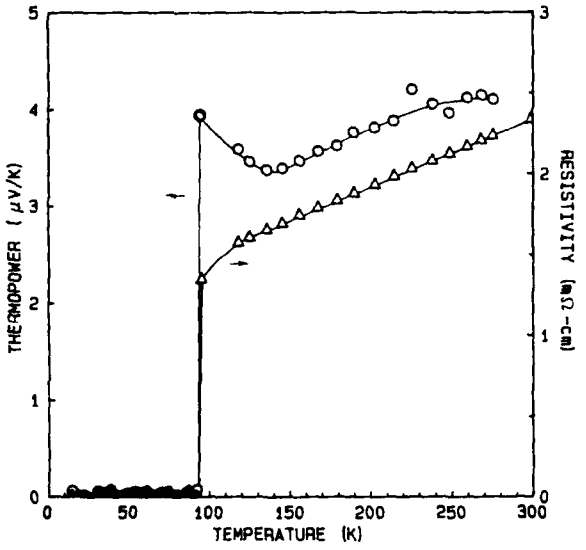

Figure 3. The resistivity (triangles) and absolute thermoelectric power (circles) for sample 1, $YBa_2Cu_3O_7$, as a function of temperature.

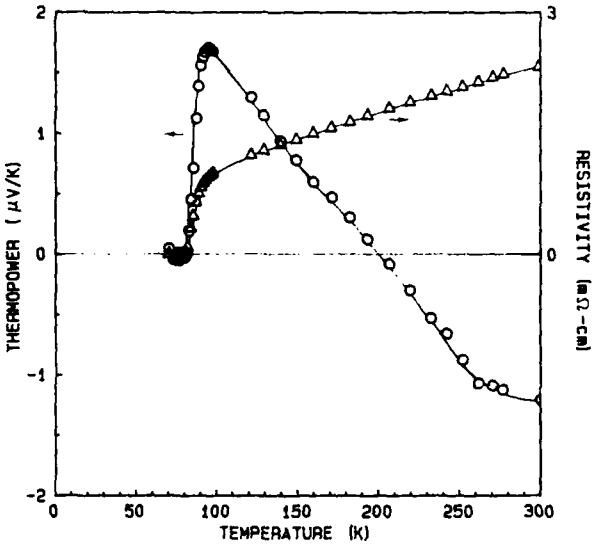

Figure 4. The resistivity (triangles) and absolute thermoelectric power (circles) for sample 2, nominal composition $Bi_2Sr_2Ca_1Cu_2O_{8+\delta}$, as a function of temperature.

The data in Figure 6 show that sample 4 is a mixed-phase sample with superconducting transitions near 110K and 80K. This may indicate that sample 4 has the composition $Bi_2Sr_2Ca_{n-1}Cu_nO_{2n+4+\delta}$ with a mixture of the n=3 and n=2 phases, respectively. The thermopower data suggest that both phases are dominated by hole-like carriers.

The resistivity versus temperature for sample 5 is illustrated in Figure 7. Sample 5 was not made in time to be included in the thermoelectric measurements. This sample has enough of the higher temperature phase that no lower transition is apparent in this measurement. The onset transition temperature is about 115K and the midpoint of the transition is 106K. Magnetization and thermoelectric power measurements on this sample are in progress and will be reported in a subsequent publication.

Discussion

The bismuth family of layered superconducting structures presents a formidable challenge to understand. The set of crystal structures represented formally as $Bi_2Sr_2Ca_{n-1}Cu_nO_{2n+4+\delta}$ may be an idealized oversimplification of the possible structures. Unlike the $YBa_2Cu_3O_7$ structure, where the correct structure is obtained by reacting the constituent materials in the desired final amounts, these bismuth materials apparently require initial compositions which are off stoichiometry. This makes it more difficult to achieve a desired composition and results in extraneous x-ray peaks due to non-reacted materials and other by-products of the synthesis. Three of the four bismuth samples described in this paper were made from different nominal compositions, they all showed distinct x-ray spectra, and they all had different transport properties. However, there are several observations which can be made. Three of the four bismuth samples showed a lower temperature superconducting transition with a midpoint in the range of 80-90K. Many samples similar to those described here show partial higher temperature superconducting transitions near 110K. As illustrated in Figure 6, sample 4 has a significant fraction of this higher temperature transition showing in both the resistivity and thermopower. Also, as shown in Figure 7, sample 5 appears to be all high temperature phase. However, the resistivity is not the best measurement to study multiphase samples. The magnetization measurements currently in progress should reveal what fraction of sample 5 is in the higher temperature superconducting phase, and how much remains, if any, in the lower temperature phase.

In all of the superconducting transitions observed, the superconductivity is due to the pairing of holes, as evidenced by the abrupt decrease in the thermopower from a positive value. The thermopower decreases to zero at the lower transition as expected. However, there are numerous known cases where the thermopower has the opposite sign of the carrier charge. The noble metals are a classic example. The measured thermopower has both positive and negative contributions, from holes and electrons, respectively, each of which can be enhanced by such effects as phonon drag and

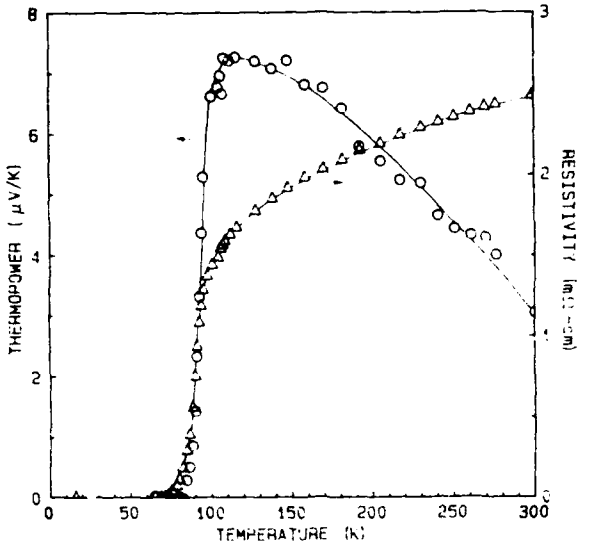

Figure 5. The resistivity (triangles) and absolute thermoelectric power (circles) for sample 3, nominal composition $Bi_2Sr_2Ca_2Cu_3O_{10+\delta}$, as a function of temperature.

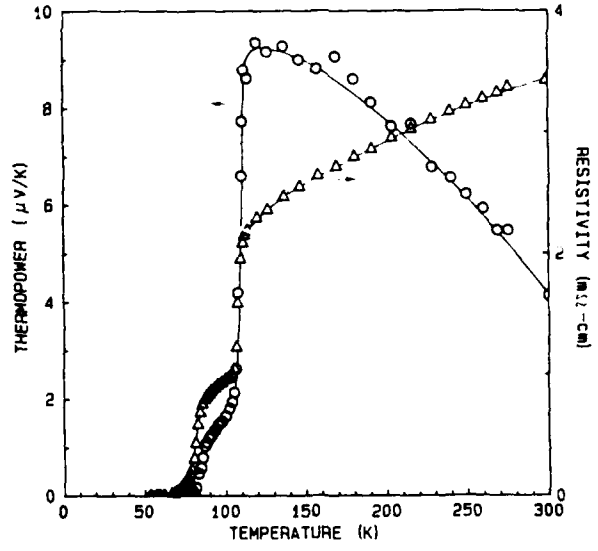

Figure 6. The resistivity (triangles) and absolute thermoelectric power (circles) for sample 4, nominal composition $Bi_4Sr_3Ca_3Cu_6O_x$, as a function of temperature.

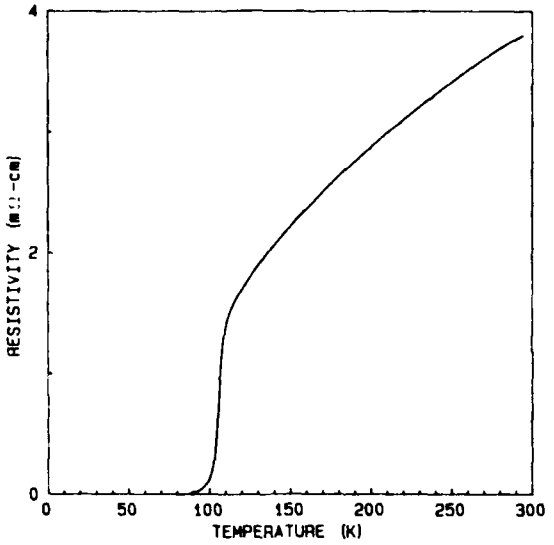

Figure 7. The resistivity for sample 5, nominal composition $Bi_4Sr_3Ca_3Cu_6O_x$, as a function of temperature.

inelastic scattering. Significant electronic contributions to the thermopower are therefore possible even though the net thermopower is positive. However, at the transition, those carriers which pair into the condensed superconducting state lose their ability to generate a diffusion-driven thermoelectric voltage. Thus, the abrupt drop in the thermopower for the mixed phase sample 4, more than the fact that the thermopower is positive, implies pairing of holes. That is, the thermopower abruptly becomes less positive or more negative in an algebraic sense, precisely at the superconducting transition because the pairing of holes diminishes their positive contribution to the diffusion thermopower. This is particularly incisive for sample 4, the mixed phase sample, because this abrupt drop takes place at the higher temperature transition, coincident with the resistance drop, even though there is no percolation path shorting the sample, which would mask the effect. Once a superconducting percolation path shorts the sample, the thermopower will go to zero independent of whether it is due to electrons or holes.

This picture is consistent with the band structure calculation mentioned in the introduction (15), where electrons are removed from the Cu-O planes leaving p-type carriers. It is these p-type carriers which give the superconductivity in this class of bismuth superconductors at both the lower and higher temperature transitions. The question to be answered then, is what acts as the sink for the transferred electrons? The bismuth cations are unlikely sites for the transferred electrons (when $\delta=0$) because the bismuth is already in its lowest valence state. However, it is possible that the transferred electrons are due to extra oxygen atoms between adjacent Bi-O layers. In this case, δ becomes finite and some Bi ions in the Bi-O planes can now be considered formally valence +5 and the Bi-O planes can then serve as a sink for electrons from the Cu-O planes. Evidence that this might be the case can be inferred from x-ray data of Tarascon *et al.* (5), showing a partial extra oxygen occupancy near 0.06, implying that $\delta=0.06$.

Thus, in this picture, the Bi-O planes function in an analogous way to the chains of Cu-O in the $YBa_2Cu_3O_7$. That is, electrons are transferred from the Cu-O planes due to the partially occupied oxygen sites in the Bi-O interplanar regions in the former material, and to the Cu-O chains in the latter. The details of the charge transfer are different, but the results are the same.

The thallium material, believed to form in a similar set of layered structures specified as, $Tl_2Ba_2Ca_{n-1}Cu_nO_{2n+4+\delta}$, is not discussed experimentally in this paper. However, one can easily conjecture that a similar transfer of electrons may occur in that material. This transfer may be greatly facilitated in the thallium compound because the thallium has a lower valence state available. Hence, the thallium cations themselves could serve as sinks for the transferred charge without the ancillary requirements of Cu-O chains, as in the yttrium material, or of extra oxygen atoms in the structure, as may be the case for the bismuth superconductors.

Literature Cited

1. Chu, C.W.; Bechtold, J.; Gao, L.; Hor, P.H.; Huang, Z.J.; Meng, R.L.; Sun, Y.Y.; Wang, Y.Q.; Xue, Y.Y. Phys. Rev. Lett. **1988**, 60 (10), 941-943.
2. Takayama-Muromachi, Eiji; Uchida, Yoshishige; Ono, Adira; Izusi, Fujio; Onoda, Mitsuki; Matsui, Yoshio; Kosuda, Kosuke; Takakawa, Shunji; Kato, Katsuo preprint submitted to Jpn. J. Appl. Phys.
3. Sheng, Z.Z.; Hermann, A.M.; El Ali, A.; Almasan, C.; Estrada, J.; Datta, T.; Matson, R.J. Phys. Rev. Lett. **1988**, 60 (10), 937-940.
4. Hazen, R.M.; Finger, L.W.; Angel, R.J.; Prewitt, C.T.; Ross, N.L.; Hadidiacos, C.G.; Heaney, P.J.; Veblen, D.R.; Sheng, Z.Z.; El Ali, A.; Hermann, A.M. Phys. Rev. Lett. **1988**, 60 (16), 1657-1660.
5. Tarascon, J.M.; LePage, Y.; Barboux, P.; Bagley, B.G.; Greene, L.H.; McKinnen, W.R.; Hull, G.W.; Giroud, M; Hwang, D.M. submitted to Phys. Rev.
6. Uher, C.; Kaiser, A.B.; Gmelin, K.E.; Walz, L. Phys. Rev. B **1987**, 36 (10), 5676-5679.
7. Uher, C.; Kaiser, A.B. Phys. Rev. B **1987**, 36 (10), 5680-5683.
8. Tranquada, J.M.; et al., Phys. Rev. B **1987**, 36, 5263.
9. Shen Z.X.; et al., Phys. Rev. B **1987**, 36, 8414.
10. Evain, Michel; Whangbo, Myung-Hwan; Beno, Mark A.; Williams, Jack M. J. Am. Chem. Soc. **1988** 110, 614-616.
11. Whangbo, Myung-Hwan; Evain, Michel; Beno, Mark A.; Geiser, Urs; Williams, Jack M. Inorg. Chem. **1988**, 27, 467-474.
12. Curtiss, L.A.; Brun, T.O.; Gruen, D.M. Inorg. Chem. **1988**, 27, 1421-1425.
13. O'Keeffe, Michael; Hensen, Staffan J. Am. Chem. Soc. **1988**, 110, 1506-1510.
14. Xiao, Gang; Cieplak, M.Z.; Gavrin, A.; Streitz, F.H.; Bakhshai, A.; Chien, C.L. Phys. Rev. Lett. **1988**, 60 (14), 1446-1449.
15. Hybertsen, Mark S.; Mattheiss, L.F. Phys. Rev. Lett. **1988**, 60 (16), 1661-1664.
16. Chaikin, P.M.; Kwak, J.F. Rev. Sci. Instrum. **1975**, 46 (2), 218-220.
17. Manual on the Use of Thermocouples in Temperature Measurement, ASTM Special Technical Publication 470, American Society for Testing and Materials, 1916 Race Street, Philadelphia, Pa. 19103, **1970**.
18. Crisp, R.S.; Henry, W.G.; Schroeder, P.A. Philos. Mag. **1964**, 10, 553-577.
19. Roberts, R.B.; Philos. Mag. **1977**, 36 (1), 91-107.

RECEIVED July 15, 1988

Reprinted from ACS Symposium Series No. 377
Chemistry of High-Temperature Superconductors II
T. F. George and D. L. Nelson, Editors